Hydrofoil sound-source origin investigation by setting the Dynamic Mode Decomposition of PIV data into Lighthill's equation

Samuel Pinson[1], Paul François[1], and Jacques-André Astolfi[1]

[1] IRENav EA 3634, BCRM Brest, École Navale C600, 29240 Brest Cedex 9

samuel.pinson@ecole-navale.fr

Abstract: *As it can affect performances, prone structural failures, disturb users, impact acoustic discretion and the whole ecosystem around, vibrations and noise of hydrodynamic lifting surfaces is a matter of great concern. Mention of discrete frequency tones from a sharp-trailing-edge airfoil at moderate Reynolds number appears in the early 70's. The phenomenon has been reconsidered very recently for aerodynamic applications and was found to originate from boundary layer velocity fluctuations at the trailing edge due to Tollmien-Schlichting waves. A recent work in the hydrodynamic tunnel of the French Naval Academy research center (IRENav) made it possible to study the flow around an hydrofoil when tonal noise emission occurs thanks to Time-Resolved Particle Image Velocimetry (TR-PIV) and laser vibrometry measurements at transitional Reynlods numbers. A Dynamic Mode Decomposition (DMD) was then used in order to extract the flow characteristics which correspond to organized vortex shedding of the wake at the tonal noise frequency. These structures show a strong coupling of the vortex shedding with the hydrofoil modal vibrations which raises the question on the origin of the emitted sound. To study the vortex-shedding sound-source hypothesis, DMD results are used as source terms in Lighthill's equation. Lighthill's tensor components are a product of velocity derivatives and thus are non-linear. Using the three modes (at 0 Hz, 197 Hz and 767 Hz) obtained by the DMD, Lighthill's tensor can be decomposed into a finite number of harmonic terms with frequencies being the combinations (sums and differences) of the three mode frequencies. Computation of the sound level from radiating components in the wavenumber domain show that the vortex shedding is not directly the origin of the perceived sound.*

Keywords: *Hydrofoil tonal noise, Particle Image Velocimetry, Dynamic Mode Decomposition, Lighthill's equation.*

1. INTRODUCTION

Noise and vibrations of hydrodynamic lifting surfaces are a matter of great concern as they can affect performance, cause structural failures, disturb users, impact acoustic discretion, and affect the surrounding ecosystem. Work conducted on airfoil tonal noise in the last decades is of great interest. Clark[3] was the first to mention discrete frequency tones from a sharp-trailing-edge airfoil at a moderate Reynolds number. Paterson *et al.*[7] also observed tonal noise on airfoils at Reynolds numbers close to 8×10^5 at a small angle of attack of $\alpha = 6^{\circ}$. Tam[10] questioned the simple Strouhal number correlation and the Kármán vortex-type organization of the wake. He suggested that the tones are generated by a self-excited feedback loop involving unstable disturbances in the boundary layer and wake flow along with a feedback of acoustic waves. Using this feedback loop model, a ladder-type evolution of the dominant frequency based on Shen[9] and Lin[5] stability curve can be drawn crossing the Strouhal law of Paterson *et al.*. In an attempt to clarify the tonal noise generation mechanism on aerofoils at a moderate Reynolds number, Nash *et al.*[6] conducted experiments on a NACA0012 aerofoil section at 6° of incidence. They showed that the ladder-type evolution of tones could be eliminated in anechoic conditions. Their results also revealed the presence of strongly amplified boundary-layer instabilities just upstream of the pressure surface trailing edge and rolling up to form a regular Kármán-type vortex street. They proposed a new mechanism for tonal noise generation based on the growth of Tollmien Schlichting instability waves amplified by inflectional profiles in the laminar shear layer. They also demonstrated, thanks to flow visualization, that the flow at the trailing edge is organized as a coherent structure. However, these studies did not take into account the hydrofoil vibrations. Watine *et al.* showed that the coexistence of two Kármán modes is responsible for the early occurrence of resonance of a blunt plate. Ducoin *et al.*[4] observed a discrete frequency excitation mechanism involving a transition on the suction side of a hydrofoil, thanks to vibratory response. Based on experiments conducted on a NACA66312 laminar hydrofoil at low angle of attack and transitional Reynolds numbers, they showed that the frequency of the boundary-layer transition mechanism can couple with some natural frequencies of the hydrofoil, leading to significant vibrations. The aim of the present study is to clarify whether or not the origin of acoustic emission on a symmetric NACA0015 hydrofoil, which generates a strong tonal noise, is due to the wake of the hydrofoil vortex street.

2. EXPERIMENT DESCRIPTION

Experiments were performed in the hydrodynamic tunnel of the French Naval Academy Research Institute (IRENav) in a square test section of $0.192m \times 0.192m$ having a honeycomb standardized inlet flow (fig. 1). An Aluminium NACA0015 section hydrofoil of 69GPa Young modulus, with constant chord of 0.1m and a span w_{foil} of 0.191m were mounted in a clamped-free configuration in a three components effort measurement system. The flow speed was regulated up to 12 $\mathrm{m\,s^{-1}}$ (i.e. a Reynolds numbers range, referred to the chord up to 12×10^5). The hydrofoil emitted an audible pure tone at 767 HZ during the experiment.
Time Resolved Particle Image Velocimetry (TR-PIV) was carried out on the hydrofoil wake with a SpeedSense 2640 Phantom camera and a 1024x400 pixel frames at 10 kHz and a Nd-Yag double cavity Laser. DynamicStudio® from Polytech® post processing was performed with an interrogation area of 8x8 pixel and 4 pixel recovery giving rise to 251x98 pixel vector fields. For each acquisition, 1000 pictures were collected over a period of 0.2s. The experiments were

performed for specific conditions of a strong hydroelastic coupling resulting in a strong pure tone emission.

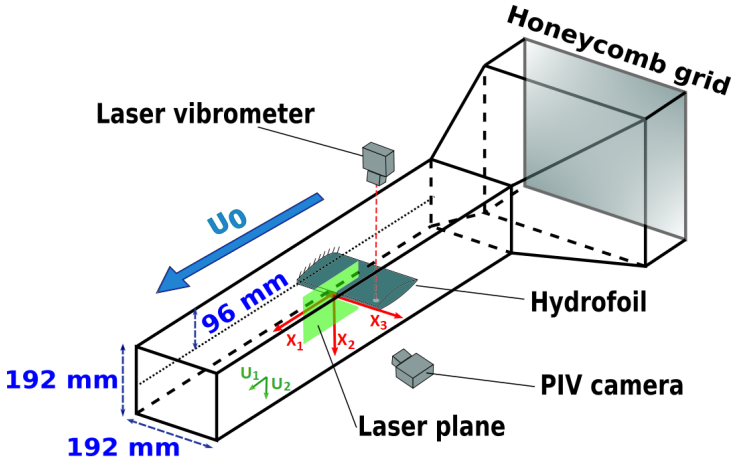

Figure 1: Clamped-free hydrofoil in the IRENav test section with PIV laser plane [11]

3. LIGHTHILL'S EQUATION ON DYNAMIC MODES

Dynamic Mode Decomposition (DMD) was performed on PIV measurements thanks to Zigunov's DMD-Wrapper algorithm [12] in order to identify wake coherent structure [8]. He showed that DMD method is able to extract dynamic information from experimental flow and can be used to describe the physical mechanisms. DMD reconstruction presented in this article is spatial TR-PIV flow speed vector associated with the frequency exhibiting the highest spatial consistency. Beside the mean flow (f_0=0 Hz mode frequency) 4 modes have been extracted by the DMD at $f_{\pm1} = \pm197$ Hz and $f_{\pm2} = \pm767$ Hz. These frequencies were found to correspond to vibration structural modes and f_2 corresponds to the pure tonal emission. fig. 2 shows horizontal velocity u_1 in the left column and the vertical velocity u_2 in the right column. Rows correspond to the mode frequencies (fields from negative and positive frequencies are added together such that the result is real valued).

DMD greatly reduces the amount of data which permits to deduce the sound field induced by the turbulence by integrating the Lighthill's equation [13] with a low computationnal cost. Indeed, the velocity field $\mathbf{u} = (u_1, u_2)$ may be reconstructed from those modes *i.e.* $u_i(t, \mathbf{x}) = \sum_{n=-2}^{2} u_i(f_n, \mathbf{x}) \mathrm{e}^{\mathrm{i}2\pi f_n t}$ (inverse Fourier transform) such that the velocity field dimension of time is reduced to 5 values (at 0, ±197 and ±767 Hz). Lighthill's equation in harmonic regime at frequency f for the fluctuation in density ρ' can thus be written in the following manner:

$$\Delta\rho'(f, \mathbf{x}) - \left(\frac{2\pi f}{c_0^2}\right) \rho'(f, \mathbf{x}) = -\frac{1}{c_0^2} \partial_{x_i x_j} T_{ij}(f, \mathbf{x}) \ , \tag{1}$$

where c_0 is the sound speed in water at rest, $T_{ij}(f, \mathbf{x}) \approx \rho_0 u_i(f_n, \mathbf{x}) u_j(f_m, \mathbf{x})$ is the approximation of Lighthill's tensor for incompressible fluid such that $f = f_n + f_m$ is a combination of 2 turbulence modal frequencies and ρ_0 is the water density. Acoustic pressure p is obtained by integration of Lighthill's equation using the 3D space Green's function:

$$p(f, \mathbf{x}) = c_0^2 \rho'(f, \mathbf{x}) = -\int_V \frac{\mathrm{e}^{\mathrm{i}2\pi f |\mathbf{x}-\mathbf{x}'|/c_0}}{4\pi \left|\mathbf{x}-\mathbf{x}'\right|} \partial_{x_i x_j} T_{ij}(f, \mathbf{x}') \mathrm{d}\mathbf{x}' \ . \tag{2}$$

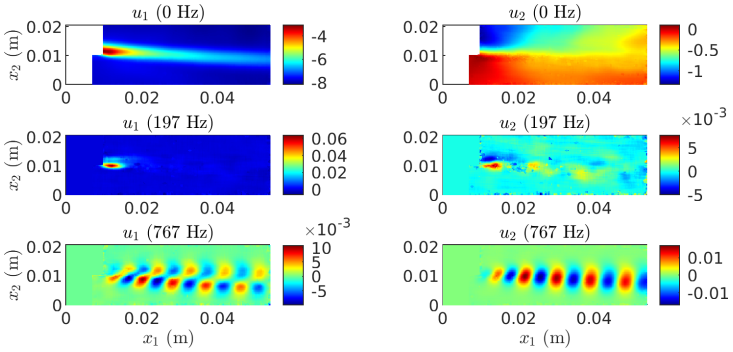

Figure 2: Velocity field real parts obtained from the DMD. Left column corresponds to the horizontal velocity, and right column corresponds to the vertical velocity. The three rows correspond to the modal frequencies (0 Hz, 197 Hz and 767 Hz). Real parts of negative frequency modes are identical (the relation between modes of different frequency signs is a complex conjugaison).

Considering that Lighthill's tensor contains products of velocities, the wave equation integral is calculated for frequencies being a combination of two modal frequencies *i.e.* $f = 0\,, \pm 197\,, \pm 394\,, \pm 570\,, \pm 767\,, \pm 964$ and $\pm\, 1523$ Hz. So the source term in Equ. 1 and 2 can thus be written more explicitly by:

$$\partial_{x_i x_j} T_{ij}(f, \mathbf{x}') = \rho_0 \sum_i \sum_j \frac{\partial u_i(f_n, \mathbf{x})}{\partial x_j} \frac{\partial u_i(f_m, \mathbf{x})}{\partial x_j} + \frac{\partial u_i(f_m, \mathbf{x})}{\partial x_j} \frac{\partial u_i(f_n, \mathbf{x})}{\partial x_j}\,, \tag{3}$$

where individual derivative terms are displayed in fig. 3. For example let's consider $\partial_{x_1 x_2} T_{12}(f = +964$ Hz, $\mathbf{x}')$, this source term component will be the product of the fields presented in {row 2, column 2} and in {row 3, column 3} added to the product of the fields presented in {row 3, column 2} and in {row 2, column 3}.

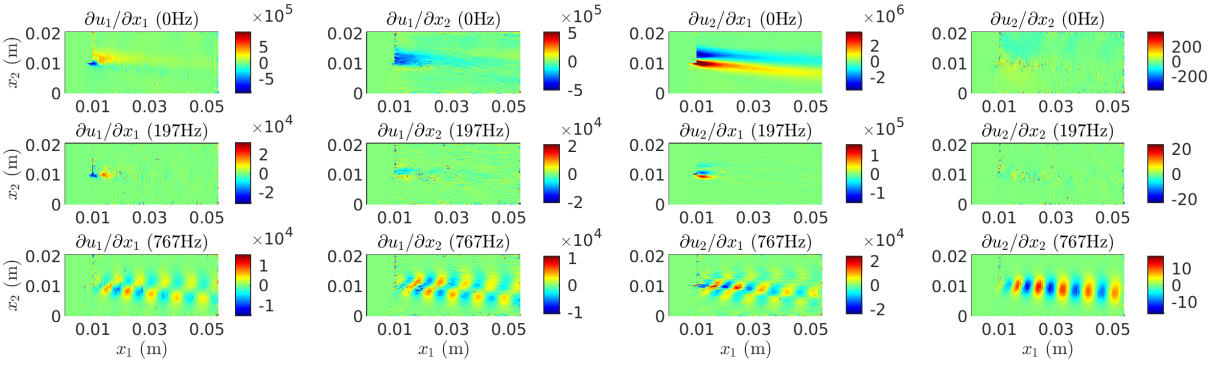

Figure 3: Velocity spatial derivative real parts of the computed modes (real parts of negative frequency modes are identical).

4. RESULTS AND DISCUSSION

For numerical integration of eq. 2, two methods have been implemented. For both, source terms along x_3 are considered constant. So integration along x_3 direction results simply in the hydrofoil width w_{foil}.

1- An approximated method considers the small domain size ($\approx 2 \times 5$ cm) compared to the wavelength (≈ 2 m at 767 Hz and ≈ 1 m at 1533 Hz). In the spatial frequency domain, and from a numerical point of view, spatial frequency is sampled at the inverse of the domain size. Thus, the only radiating component is included in the sample at null spatial frequency. Thus the sound pressure at 1 m is simply:

$$p(f) = w_1 \times w_2 \times w_{foil} \times \partial_{x_i x_j} T_{ij}(f, k_1 = 0, k_2 = 0)/4\pi \, , \tag{4}$$

where $T_{ij}(f, k_1, k_2)$ is the 2D spatial Fourier transform of $T_{ij}(f, \mathbf{x})$, $k_{1,2}$ are the horizontal and vertical wavenumbers and $w_{1,2}$ are the measured field lengths. Sound pressure level thus obtained (in db *re* 1μPa) for the different frequencies are presented in fig. 4 with red bars. Besides, looking at source terms in the spatial frequency domain permits to notice that these spatial spectrum are very narrow. This gives the opportunity to estimate a noise standard deviation σ_T in spectral region where signal is obviously absent. The obtained result for the acoustic pressure field can then be compared to a pressure field obtained with the data noise level:

$$p_{noise}(f) = w_1 \times w_2 \times w_{foil} \times \sigma_T/4\pi \, , \tag{5}$$

to check the pertinence of the calculated pressure field obtained from eq. 4. Sound pressure levels obtained from the estimated noise in the spatial frequency domain are presented in fig. 4 with orange bars.

2- To account for potential multipolar source terms that might be missed by the approximation of the first method, the numerical evaluation of the integral is necessary. As for the first method, the velocity field is considered constant over x_3 and integration over it gives w_{foil}. Then integration over x_1 and x_2 is performed for $\mathbf{x}$ in a far field circle in the plane $(x_1, x_2, x_3 = 0)$. The computed acoustic pressure level is then brought back to a 1 m distance from the domain center. Maximum value on the circle surrounding the domain for the sound pressure levels (fluctuations do not exceed 1 dB) are presented in fig. 4 with blue bars.

From fig. 4, one can see a good match between the results obtained from numerical evaluation

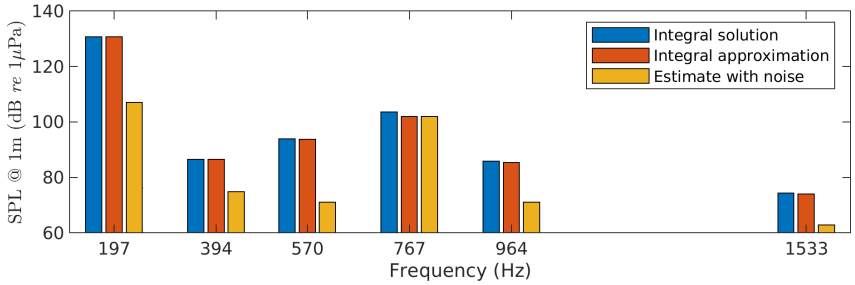

Figure 4: Sound pressure levels obtained with different methods..

of the integral in eq. 2 and its approximation (eq. 4). Nevertheless the control values obtained with data noise level (eq. 5) show similar results as for the calculated pressure meaning that they are not significant. Acoustic measurement near the tunnel during the experiment (not presented here) showed a single frequency (that could be heard) at 767 Hz. In conclusion, it is highly unlikely that this perceived sound was generated by the hydrofoil vortex street. To get an order of magnitude of the sound level that would result in the air from our calculated results, one might subtract 90 dB from the results in fig. 4 (by applying a water-to-air transmission coefficient and changing the reference level from 1μPa to 20μPa). It means that the heard tone level at 767 Hz would be $\approx$15 dB, which is very low and well below the ambient noise level around the tunnel.

5. CONCLUSION

The pure tonal sound emitted from a metallic hydrofoil for specific hydroelastic coupling conditions has been experimentally examined by TR-PIV measurement, Dynamic Modal Decomposition analysis and Ligthill's analogy. It is unlikely that hydrofoil vortex street is at the origin of the emitted tonal noise. Most plausible hypothesis for the sound genesis is through mechanical vibration of the structure. Nevertheless, pressure side transition is still to be investigated to fully discard the hydro-acoustic hypothesis.

REFERENCES

[1] H. Arbey, J. Bataille: Noise generated by airfoil profiles placed in a uniform laminar flow, *Journal of Fluid Mechanics* **134** 33–47 (1983)

[2] W.K. Blake: Excitation of plates and hydrofoils by trailing edge flows. *Journal of Vibration, Acoustics, Stress, and Reliability in Design* **106** 351–363 (1984)

[3] L.T. Clark: The radiation of sound from an airfoil immersed in a laminar flow, *Journal of Engineering Power* **93** 366–376 (1971)

[4] A. Ducoin, J.-A. Astolfi, M.-L. Gobert: An experimental study of boundary-layer transition induced vibrations on a hydrofoil, *Journal of Fluids and Structures* **32** 37–51 (2012)

[5] C.-C. Lin: On the Stability of Two-Dimensional Parallel Flows, *Quarterly of Applied Mathematics* **3** 117–142 (1945)

[6] E.C Nash, M.V. Lowson, A. McAlpine: Boundary-layer instability noise on aerofoils, *Journal of Fluid Mechanics* **382** 27–61 (1999)

[7] R.W. Paterson, W. Robert, P.G Vogt, M.R Fink, C.L. Munch: Vortex noise of isolated airfoils, *Journal of Aircraft* **5** 296–302 (1973)

[8] P.J Schmid: Dynamic mode decomposition of numerical and experimental data, *Journal of fluid mechanics* **656** 5–28 (2010)

[9] S.F Shen: Calculated amplified oscillations in the plane Poiseuille and Blasius flows, *Journal of the aeronautical sciences* **21** 62–64 (1954)

[10] C.K.W Tam: Discrete tones of isolated airfoils *The Journal of the Acoustical Society of America* **6** 1173–1177 (1974)

[11] Y. Watine, C. Gabillet, B. Lossouarn, J.F Deü, J.A Astolfi: Vortex-induced vibrations of a cantilevered blunt plate: POD of TR-PIV measurements and structural modal analysis *Journal of Fluids and Structures* **117** 103832 (2023)

[12] F. Zigunov: Dynamic Mode Decomposition DMD-Wrapper, MATLAB Central File Exchange, (2021).

[13] M.J. Lighthill: On sound generated aerodynamically I. General theory, *Proceedings of the Royal Society of London. Series A. Mathematical and Physical Sciences* **211**(1107) 564–587 (1952)